JOURNAL OF SOLID STATE CHEMISTRY 63, 179–190 (1986)

# TEM Study of Interfacial Relationships in the $V_2O_5$–$TiO_2$(Anatase) System

A. VEJUX* AND P. COURTINE†

*Service d'Analyse Physico-Chimique and †Département de Génie Chimique, Université de Technologie de Compiègne, B.P. 233
60206—Compiègne, France

Received July 8, 1985; in revised form November 13, 1985

A direct study of interfacial relationships in the $V_2O_5$–$TiO_2$(anatase) system is carried out with specimens consisting of $V_2O_5$ nucleated from the vapor phase on commercial anatase crystallites. The anatase-supported $V_2O_5$ as opposed to pure $V_2O_5$ proved highly unstable under the electron beam and successive structural steps were observed. Consequently the characterization of the elusive $V_2O_5$–$TiO_2$ interface by electron microscopy was not possible in general. In a few specimens, however, there was evidence of interfacial coherence. The crystallographic fit leading to the coherence is believed to be responsible for the unstability observed. An earlier assumption relating the catalytic behavior of the $V_2O_5$–$TiO_2$(anatase) system to a crystallographic fit is thus reinforced.

## Introduction

The aim of the present work was to collect through transmission electron microscopy (TEM) direct information on structural relationships in the $V_2O_5$–$TiO_2$ (anatase) system, in continuation of a previous research (*1*), which suggested that a crystallographic fit between these two oxides gives rise to preliminary conditions for the remarkable reactivity and catalytic behavior of that system.

It is a well known fact that many mild oxidation reactions of industrial importance (*2–9*) are actively and selectively catalyzed by $V_2O_5$ oxide supported on $TiO_2$(anatase) (0.2 to 7 mole%). The reactivity of the system has been extensively studied (*1, 10–15*), and, when the V and Ti ions are in $V^{5+}$ and $Ti^{4+}$ valence states, no evidence of a bulk compound resulting from a solid–solid reaction has ever been reported.

In this context, we felt it necessary to study as a priority the morphology of $TiO_2$(anatase) and $V_2O_5$, and possibly their interfacial relationships (*16*). On the basis of microgravimetric and X-ray diffraction experiments carried out at low temperature (600°C) and under pure nitrogen, we established earlier that the system simultaneously and "topotactically" undergoes a reduction of $V_2O_5$ and the transformation of anatase into rutile, whereas, if one takes each oxide separately, neither phenomenon occurs (*1, 17*). In such a synergetic effect only a considerable lowering of the potential barrier could allow for the necessary electronic and vibrational transfers. We thus were led to postulate the existence of a coherent interface, at short or long range,

0022-4596/86 $3.00

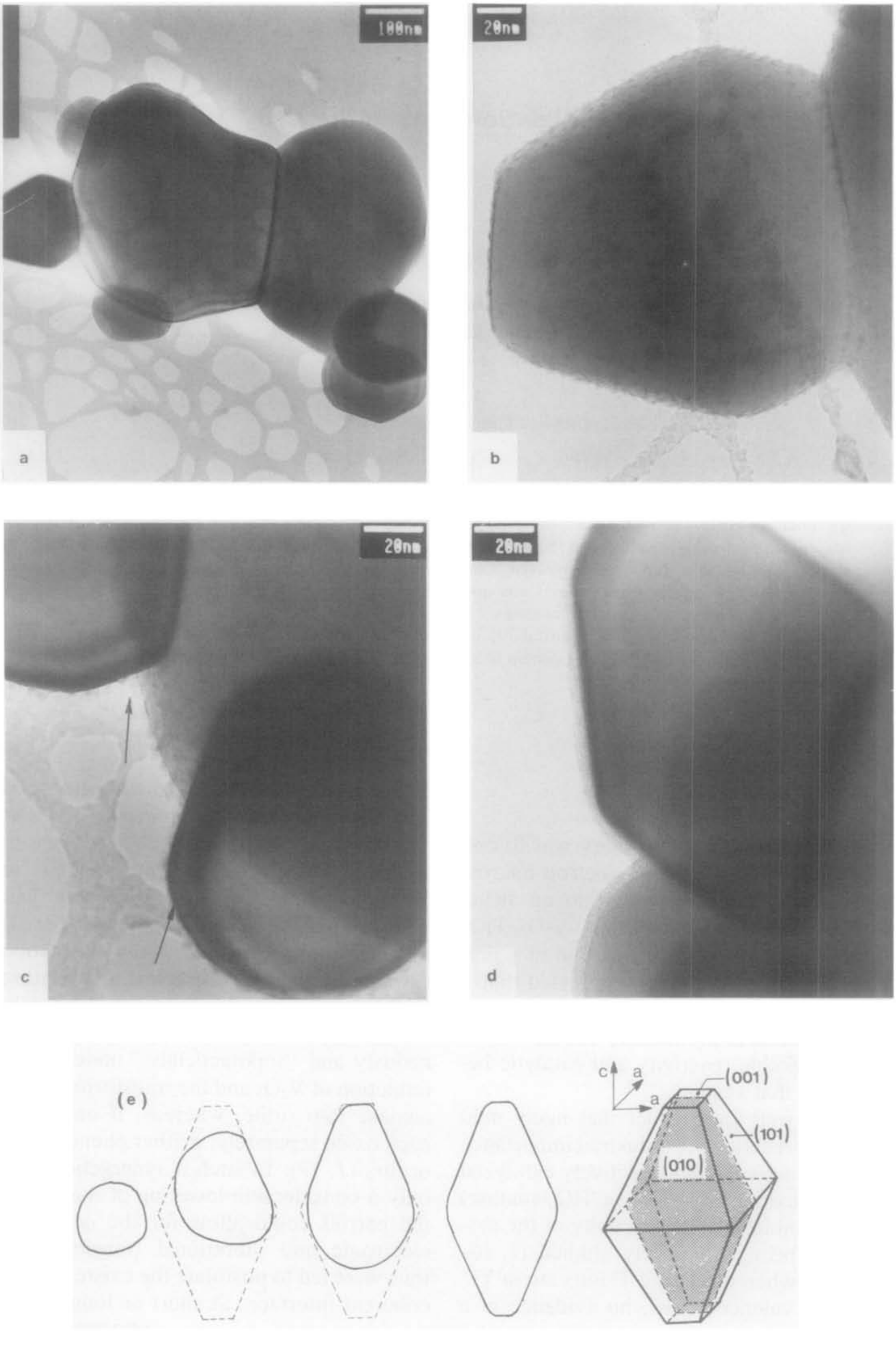
100nm
a
20nm
b
20nm
c
20nm
d
(e)
c
a
a
(001)
(101)
(010)

between the two oxides (*18a*). Our model was further strengthened, since $AlNbO_4$ and $GaNbO_4$, which present with $V_2O_5$ the same crystallographic relationship as $TiO_2$-anatase, were shown later to have, when used as support, the same effect on $V_2O_5$, under nitrogen and comparable temperature—or under catalytic conditions as well (*18b*).

Some discussions in the literature concern $TiO_2$ preparations covered with monolayers of $V_2O_5$, and interesting catalytic performances have been reported (*6–8, 14, 15*). Whether the performances still remain in the long run is not firmly established and is even being questioned (*19*). Examples with a few $V_2O_5$ molecular layers were also found to be as, or even more effective (*6–8, 13–15*). At any rate, in those cases the surface potential due to $TiO_2$ is so strong that atomic environments in the "two-dimensional" $V_2O_5$ are greatly distorted. However, when the number of layers increases, the distorsion of the $V^{5+}$ ion coordination gradually decreases, and the structure of the deposited $V_2O_5$ becomes closer to the bulk structure.

All these facts have prompted us to relate the reactivity of the heterogeneous $V_2O_5$–$TiO_2$(anatase) system to a strained but coherent interface between two crystalline phases (both of them thick enough to possess nearly bulk properties), since on the other hand conventional, efficient $V_2O_5$–$TiO_2$(anatase) catalysts are generally of the multilayer type.

With the purpose of giving our interpretation direct evidence, and thereby getting a better understanding of the *synergetic effect* of $V_2O_5$ supported on anatase, we prepared a $V_2O_5$–$TiO_2$(anatase) system presenting the essential morphologic and crystallographic features of our model (*1*), and simultaneously meeting the high-resolution electron microscopy requirements. We report and discuss here the results of that TEM investigation.

## Experimental

Basically the $V_2O_5$–$TiO_2$ specimens were obtained by nucleating $V_2O_5$, through vapor phase transport, on single crystalline anatase substrate. We consider three series of specimens (I, II, and III). Series I deals with commercial anatases (Société Tahnn & Mulhouse, Tioxide International Ltd., Bayer), characterized by a 7- to 9-$m^2/g$ specific area, and the typical impurity content: $\leqq 1$ wt% $V_2O_5$, $\leqq 0.5$ wt% $P_2O_5$, $\leqq 0.3$ wt% $K_2O$, and $\leqq 100$ ppm $Cl^-$.

Vapor phase-grown $V_2O_5$ platelets compose series II. They were prepared from 1 mg of powdered $V_2O_5$ (Merck-France S.A.), loaded at one end of silica ampoules 10 cm long and with 0.8 cm inside diameter. The evacuated ampoules were placed in a horizontal furnace, with the charge toward the higher temperature zone (900°C). Within 24 hr vaporized $V_2O_5$ gradually condensed at the ampoule wall in a cooler zone (about 600°C) under the form of very small and thin single-crystalline platelets.

The specimens of series III consisting of crystalline $V_2O_5$ nucleated on anatase substrate were prepared in a way very similar as specimens II. The only difference was the presence of traces of anatase (specimen I) on the inside wall of the ampoules, so that $V_2O_5$ had a chance to condense on anatase as well as on the ampoule wall. Different growth times were used in an attempt to

FIG. 1. $TiO_2$(anatase) crystallites. (a–d) Electron micrographs of typical crystallite morphology (specimens I) (arrows indicate lattice fringe directions). (e) Schematic diagram showing crystallite growth at successive stages (at right, one of the natural habits of $TiO_2$(anatase) crystal, evoked by specimens I).

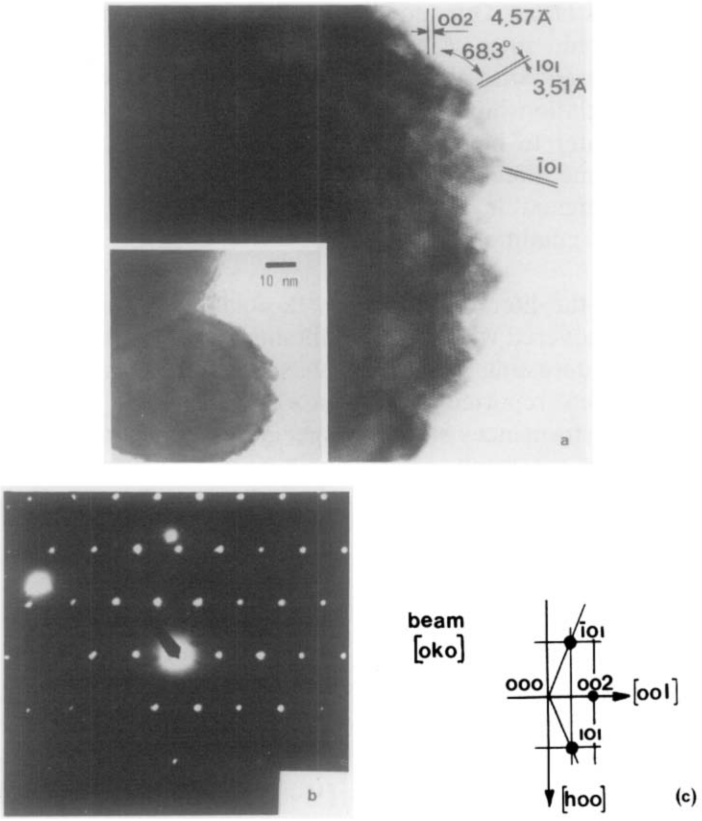

FIG. 2. $TiO_2$(anatase) crystallite analyzed by lattice imaging and electron diffraction. (a) Electron micrograph showing (101) ($\bar{1}$01), and (002) lattice images, with indication of lattice spacings and angle (insert at lower magnification gives an overall view of the crystallite). (b) Corresponding electron diffraction pattern (correctly oriented with respect to the micrograph). (c) Schematic indexing.

vary the amount of $V_2O_5$ deposited on anatase particles.

The specimens dispersed on holey carbon grids were observed with a JEOL 1200EX electron microscope operated at 120 kV.

## Results and Discussion

### *$TiO_2$(Anatase)(Specimens I)*

The anatase specimens observed were found to be constituted of scale-like crystallites isolated or clustered. As illustrated in Fig. 1, these small single crystals, roughly ranging from 50 to 500 nm in diameter and 10 nm thick or less, are still close to the nucleation phase attested by rounded contours; nevertheless, some of them exhibit to a certain degree the morphology of natural anatase crystals, namely a truncated octahedron elongated along the *c* axis (*20*).[1]

Analysis by electron diffraction and lattice imaging (Fig. 2) shows the small scale-like crystallites to have their normal approximately in the [010] direction (Fig. 3a). It does not result that they are merely thin (010) cuts in the anatase octahedron: tilting about the [101] direction rather suggests a lentil-shaped form (Fig. 3b); we assume however the surface to be vicinal to (010).

---

[1] $TiO_2$ anatase: tetragonal S.G.: $I4_1/amd$; $a = 3.785$ Å, $c = 9.514$ Å.

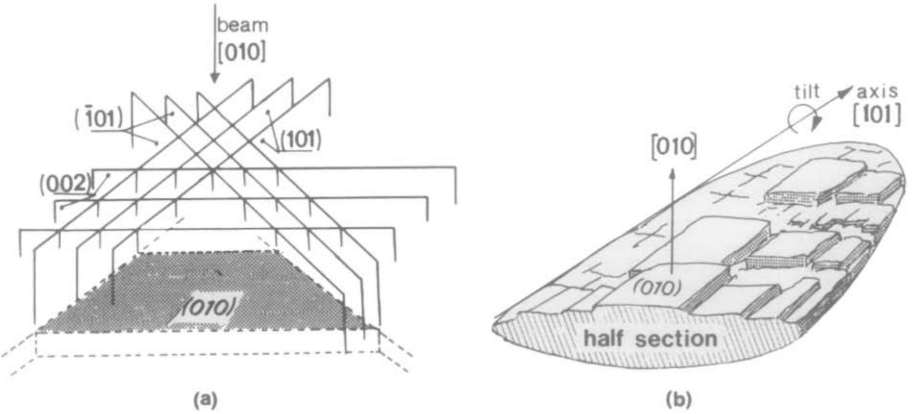

FIG. 3. $TiO_2$(anatase): crystallite modelization. (a) Plane families in a scalelike anatase crystallite found in Fig. 2a to be parallel to the electron beam. In broken line, indication of an idealized crystallite. (b) More realistic view (half-section) of an anatase crystallite, schematizing the (010) plane segments vicinal to the surface

In other words we consider that in these anatase crystallites, inspite of their complex shape, the major part of the exposed surface corresponds to (010) plane.

Commercial anatases (of the same kind used to support $V_2O_5$ in industrial catalysts) were therefore considered as adequate single crystalline substrate for our preparation, since (010) is precisely one of the two anatase planes—the other being (001)—assumed in our model (*1*) to be interfaced with $V_2O_5$.

### $V_2O_5$ (*Specimens II*)

The sole purpose of preparing vapor-grown $V_2O_5$ was to make sure that our apparatus and procedure yielded lamellar, elongated microcrystals, in accordance with the normal $V_2O_5$ crystal habit, namely a rectangular prism (20).[2] The results gathered in Fig. 4 confirmed it to be so. These specimens were found to be very stable under a standard TEM electron beam in agreement with the literature (*22–25*).

### $V_2O_5$-*Covered Anatase* (*Specimens III*)

The preparation of specimens III aimed at determining to what extent $V_2O_5$ nucleating and growing directly on (010) anatase would follow our model (partly reproduced in Fig. 5).

Most specimens III, as opposed to specimens I and II, proved extremely sensitive to the electron beam. Within seconds drastic changes were observed to occur, as if the specimens first melted, then recrystallized with the formation of a checkered texture, then rapidly sublimated and disappeared altogether (sequence of micrographs in Figs. 6d,e).

Clearly this behavior was due to the "coupling" of $V_2O_5$ and $TiO_2$(anatase) since each component is stable when taken separately, and constituted a manifestation, at microscopic level, of the remarkable reactivity of the $V_2O_5$–$TiO_2$(anatase) system. Under such conditions the characterization of the interface by electron microscopy and electron diffraction understandably becomes rather problematical.

*Observation of unstable specimens* (*general case*). In most instances, the specimens were found to present contours simi-

---

[2] $V_2O_5$: orthorhombic S.G.: $V_h^{13}$ *Pmmn*; $a = 11.51$ Å, $b = 3.56$ Å, $c = 4.37$ Å. (In previous papers (*1, 17*), we used the nowadays less-common Bachmann's notation (*21*), where *b* and *c* are permuted.)

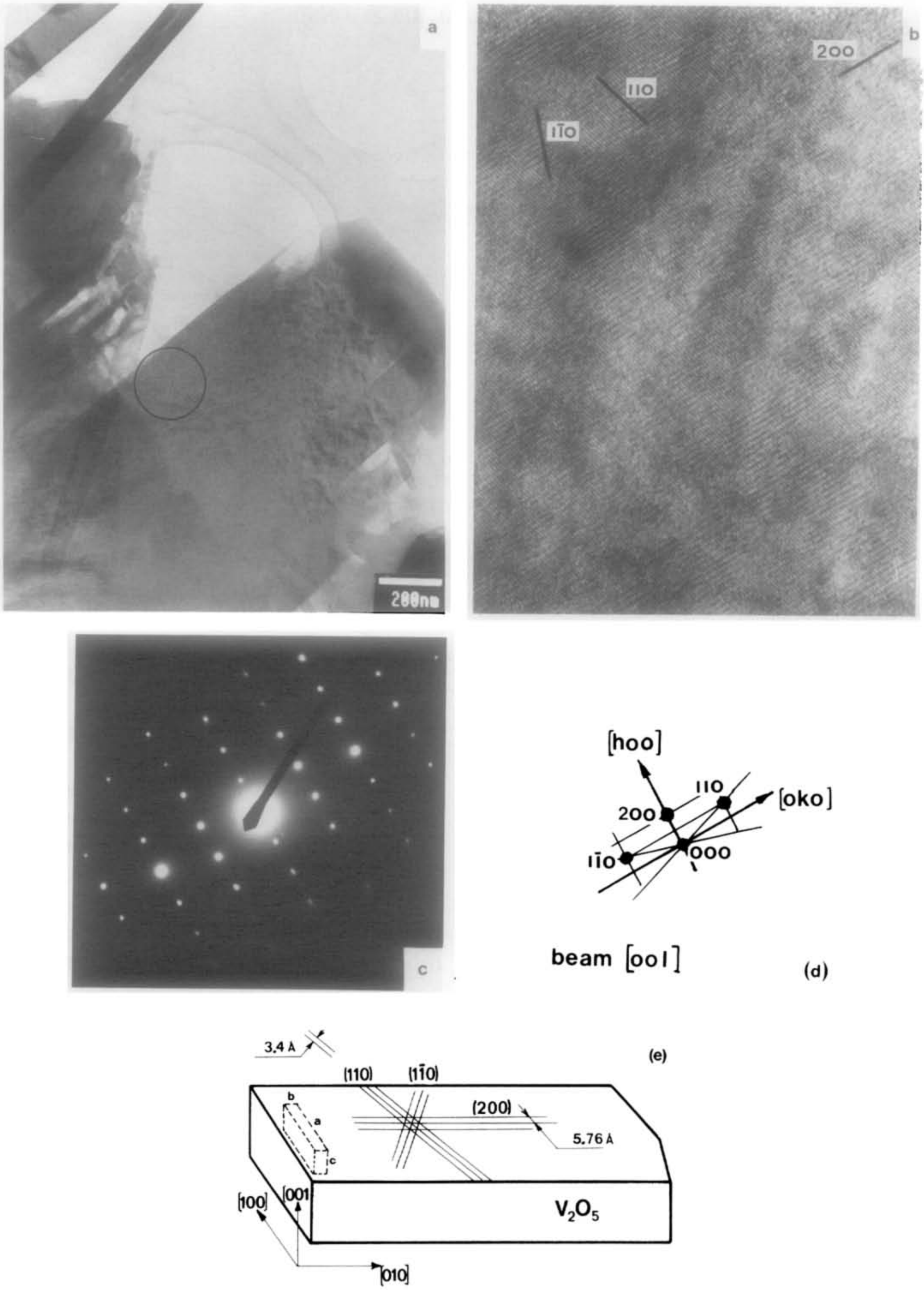

FIG. 4. $V_2O_5$ electron micrographs and crystallite modelization. (a) Crystallites with various widths (notice microdomains in circle). (b) Enlargement showing (110) ($1\bar{1}0$), and (200) lattice images. (c) Electron diffraction pattern (correctly oriented). (d) Schematic indexing. (e) Natural habit of $V_2O_5$ crystal (exhibited by specimens II).

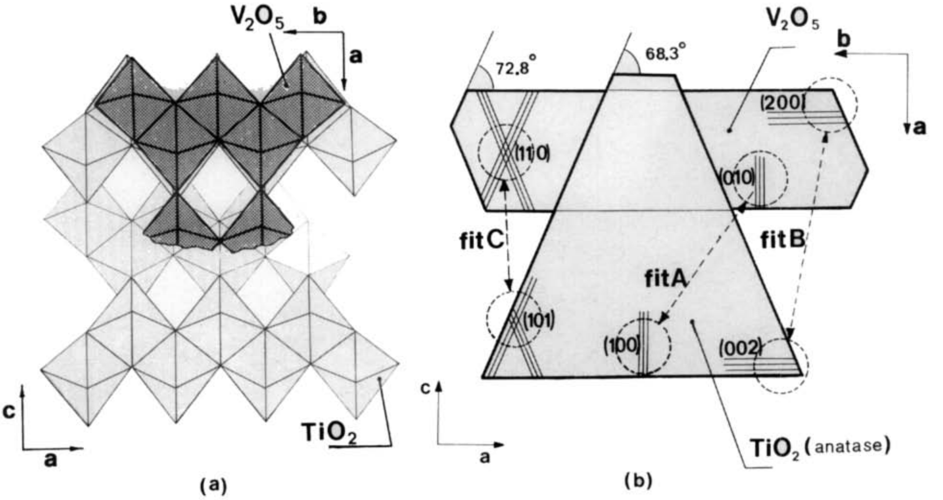

FIG. 5. (001)$V_2O_5$–(010)$TiO_2$(anatase) crystallographic fit (a) visualization of the predicted crystallographic fit in real dimensions, as already presented in Ref. (*1*). (b) Diagram and values of the three most important lattice fits: (A) (010)/(100) 6%; (B) (200)/(002) 19%; (C) (110)/(101) linear 3.5%; angular 6.4%.

lar to those of pure anatase particles (such as in Fig. 6c) but they seemed to "glitter" under the electron beam exhibiting no fixed details but a fluidlike mobility—as opposed to pure anatase particles, which are stable. In the diffraction mode, one observed rapidly changing patterns, and the photographs snapped during the process reveal various degree of disorder and streaking, indicative of structural transition. Behind the disorder, however, one detects quite often a trend toward an ordered spot configuration different from $V_2O_5$ or $TiO_2$(anatase) diffraction pattern, as in Fig. 8a and particularly Fig. 8b. The new structure, though incompletely characterized, seems from the data already available to be a superstructure, but in a higher degree of reduction than that observed in $V_2O_5$ by several authors—and shown to be $V_4O_9$ (*22–25*). (In the context of our study, that is, from the catalysis point of view, it is somewhat secondary that this superstructure is not yet completely identified, all the more because its nature may depend on the ambiant conditions—temperature, vacuum, etc.)

As mentioned above, it happened that a checkered texture formed after an exposure to the electron beam of 1 or 2 min. In the corresponding electron diffrations a rutile-like configuration becomes apparent possibly ascribable to a $V_xTi_{1-x}O_2$ solid solution. It is of interest to recall that the transformation anatase → rutile is activated by the reduction of $V_2O_5$ (*1, 17*).

*Observation of metastable specimens.* In few cases, hardly representative in terms of statistics, one observed crystalline $V_2O_5$ distinctly attached to $TiO_2$(anatase) particles (Figs. 6a–b, 7a). Such specimens were generally found to be stable under the electron beam. By inspection, the relative orientation appears, within reasonable accuracy, to be in agreement with the model Fig. 5b, namely

$$[010]V_2O_5 \;//\; [100]TiO_2(\text{anatase}) \quad \text{and} \quad [100]V_2O_5 \;//\; [001]TiO_2(\text{anatase}).$$

In Fig. 7a the electron diffraction seems to be the almost exact superimposition of the diffractions from both $V_2O_5$ and $TiO_2$(anatase), oriented according to the model (Fig-

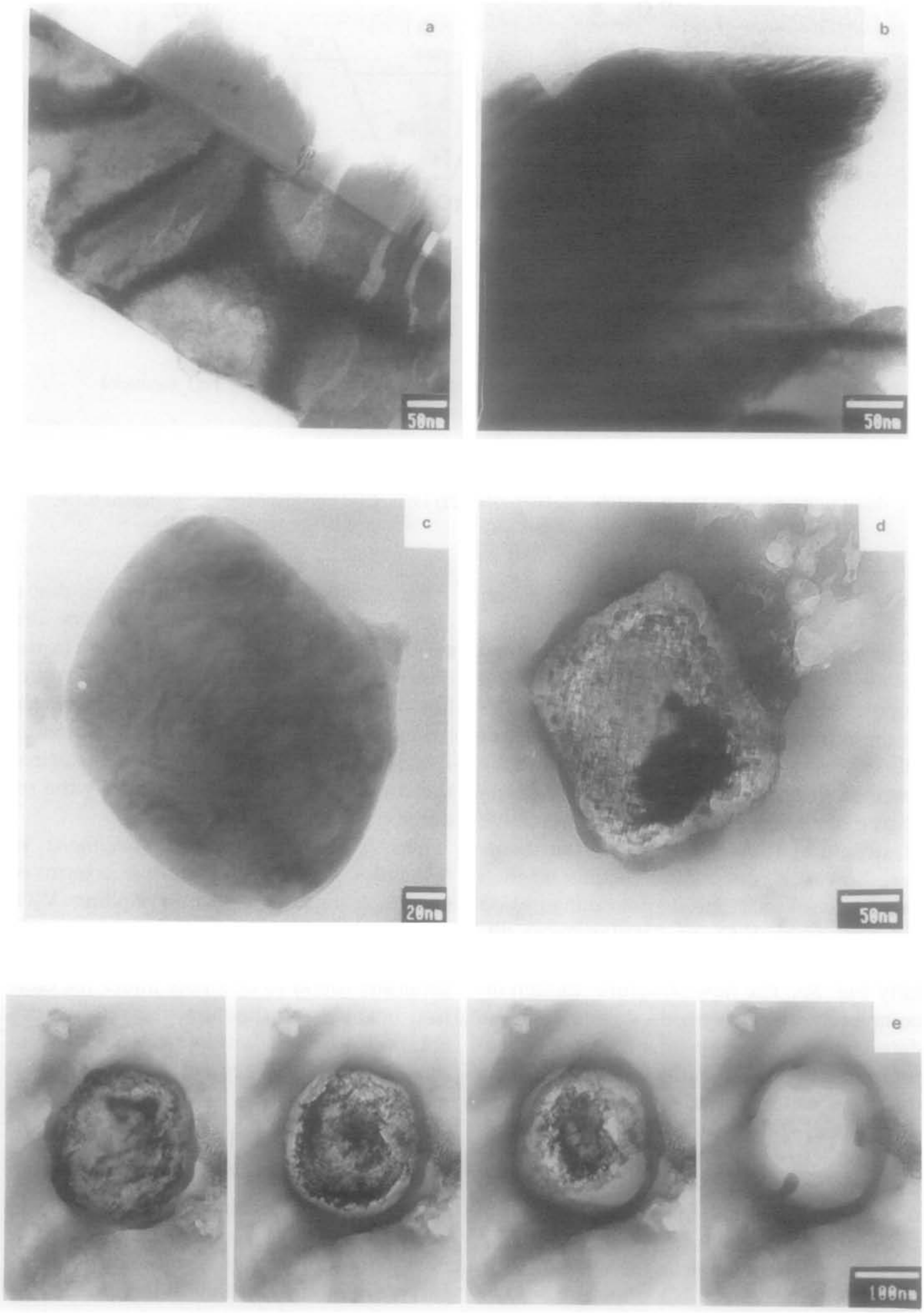
a
50nm
b
50nm
c
20nm
d
50nm
e
100nm

ure 5b). If we refer to the different fits[3] between the crystallographic structures of the $V_2O_5$–$TiO_2$(anatase) system for the two projections of interest, the nearly identical spacing between rows of diffraction spots corresponds to the good fit (A), whereas the poor fit (B) in the perpendicular direction, results in two kinds of spots: some regular and intense spots clearly belong to $V_2O_5$, whereas the others, weaker and more disordered, seem to be ascribable to $TiO_2$(anatase). Furthermore the two intense symmetrical spots nearest to the center would correspond to (110), $(\bar{1}\bar{1}0)V_2O_5$ and (101), $(\bar{1}0\bar{1})TiO_2$(anatase), the doublets in symmetrical position being assigned to the conjugated planes, with the implication that the relative orientation of the two crystals is exactly along $[110]V_2O_5$, $[101]TiO_2$(anatase), a misorientation resulting in the $[\bar{1}01]TiO_2$(anatase) direction due to the angular misfit (assumption reinforced by a small rotation of these doublets with respect to the rows of spots).

These cases are rare indeed, but they may correspond to an accidental metastability, the normal behavior being an immediate evolution under the electron beam. Then they would represent a "quenched" step usually invisible because of the unstability. This assumption implies that a *coherent* interface initially exists in the $V_2O_5$–$TiO_2$(anatase) couples but disappears as soon as the resulting synergy sets in.

The electron diffraction in Fig. 7b might be an illustration of such a transient situation: taken from an "unstable" specimen, and accordingly quite disordered, it bears nevertheless the traces of $V_2O_5$–$TiO_2$(anatase) orientation.

## Interpretation

The assumption just made resembles a dilemma: because of the coherence of the interface, the interface cannot be observed and its coherence cannot be stated.

On the basis of the various data, however, one can speculate that as soon as vanadia adsorb on $(010)TiO_2$(anatase), as in the preliminary step of an "epitaxy" (inasmuch as the classical concept of epitaxy is relevant at all in that context of reactive solids), an interfacial interaction develops making the supported $V_2O_5$ very different in its physical properties from pure $V_2O_5$.

It could be in particular that the melting temperature of supported $V_2O_5$ be considerably lowered, hence the glittering fluidity under the electron beam. Subsequently, new phases would form such as superstructures or even solid solutions of $V_2O_5$–$TiO_2$, themselves subject to rapid sublimation under the beam.

Incidentally, these considerations may be paralleled with the concept as yet ill-understood of "surface wetting" appearing in reports on $V_2O_5$ monolayers "molecularly epitaxied" onto $TiO_2$(anatase) (*31*).

It may be added also in a final remark that to account for similar transformations, Anderson (*26*) invoked place exchange between oxygen atoms and vacancy sites producing *fluctuation waves of composition*. In the case of $V_2O_5$ supported on $TiO_2$(anatase) the relaxation of $V_2O_5$ would be con-

---

[3] Crystallographic fit defined by: $200(d_i - d_j)/(d_i + d_j)$ $d_i$, $d_j$ corresponding lattice spacings.

FIG. 6. $V_2O_5$ vapor deposited on $TiO_2$(anatase) crystallites. (a,b) $V_2O_5$ crystal grown on $TiO_2$(anatase) particles (notice relative orientation of the crystals corresponding to model Fig. 5b). (c) $TiO_2$(anatase) particle actually covered with $V_2O_5$ (as evidenced by its glittering behavior under the electron beam, and by its diffraction pattern (Fig. 8b) different from that of pure anatase). (d) Specimen gradually "sublimated" under the electron beam (notice the checkered texture). (e) Sequence of micrographs showing complete "sublimation" (about 15 sec between each picture; electron beam intensity corresponding to normal observation and photography conditions).

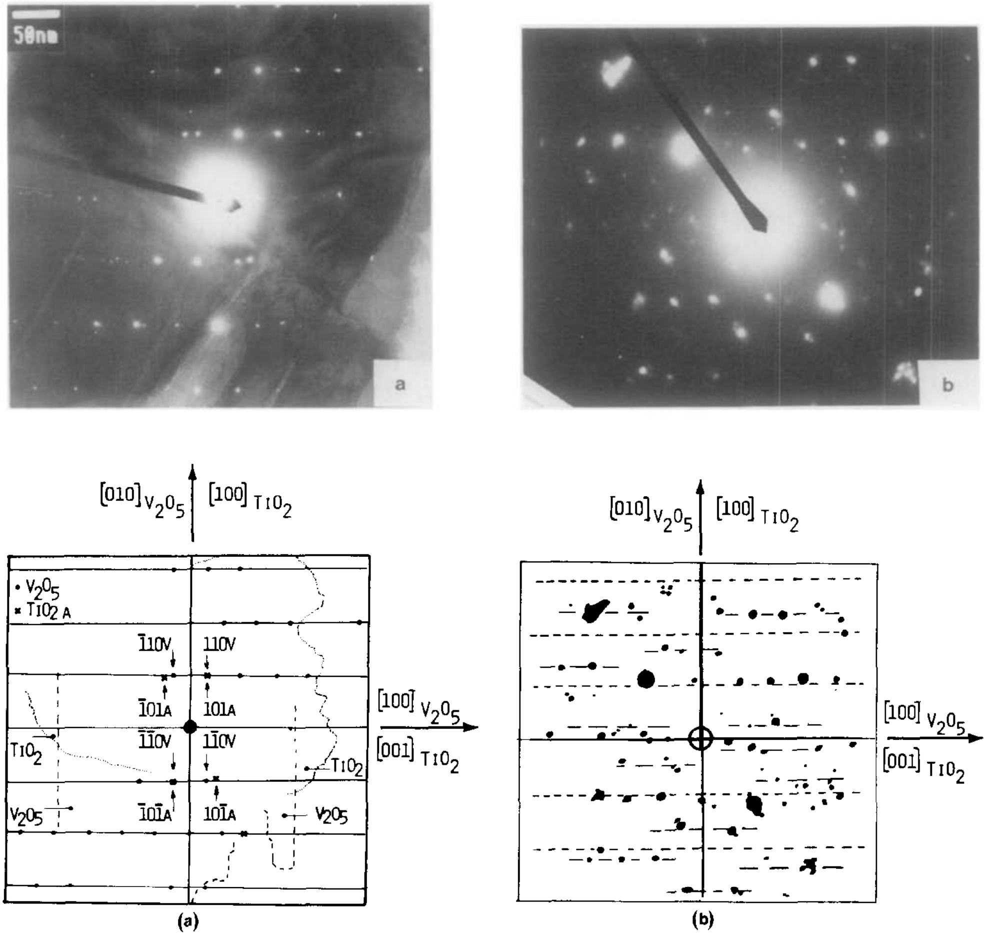

FIG. 7. Typical electron diffraction patterns from $V_2O_5$–$TiO_2$(anatase) system (specimens III). (a) Almost exact superimposition of diffraction patterns from $V_2O_5$ and $TiO_2$(anatase) oriented in accordance with model Fig. 5b (good fit A results in regularly spaced rows of spots, poor fit B results in two series of spots within rows, as discussed in text). Indicated in broken lines, schematic contours of the crystal couple (after 32° rotation correction). (b) This pattern, from an *unstable* specimen, though quite disordered, bears the traces of $V_2O_5$–$TiO_2$(anatase) orientation.

siderably enhanced by the interfacial elastic stress due to coherence (*1, 26–30*).

## Conclusion

TEM observation showed that commercial anatases (commonly used in industrial catalysts) essentially present the (010)-anatase plane in surface. As a result they constitute an adequate $TiO_2$ support in the preparation of a $V_2O_5$–$TiO_2$(anatase) system, corresponding to the crystal couple theoretically studied earlier.

Specimens obtained by direct nucleation of $V_2O_5$ onto (010)anatase plane were found to be very unstable under the electron beam, whereas pure, unsupported $V_2O_5$ under the same conditions is stable. Clear-cut epitaxial deposition of $V_2O_5$ could not be established except in rare cases. On the

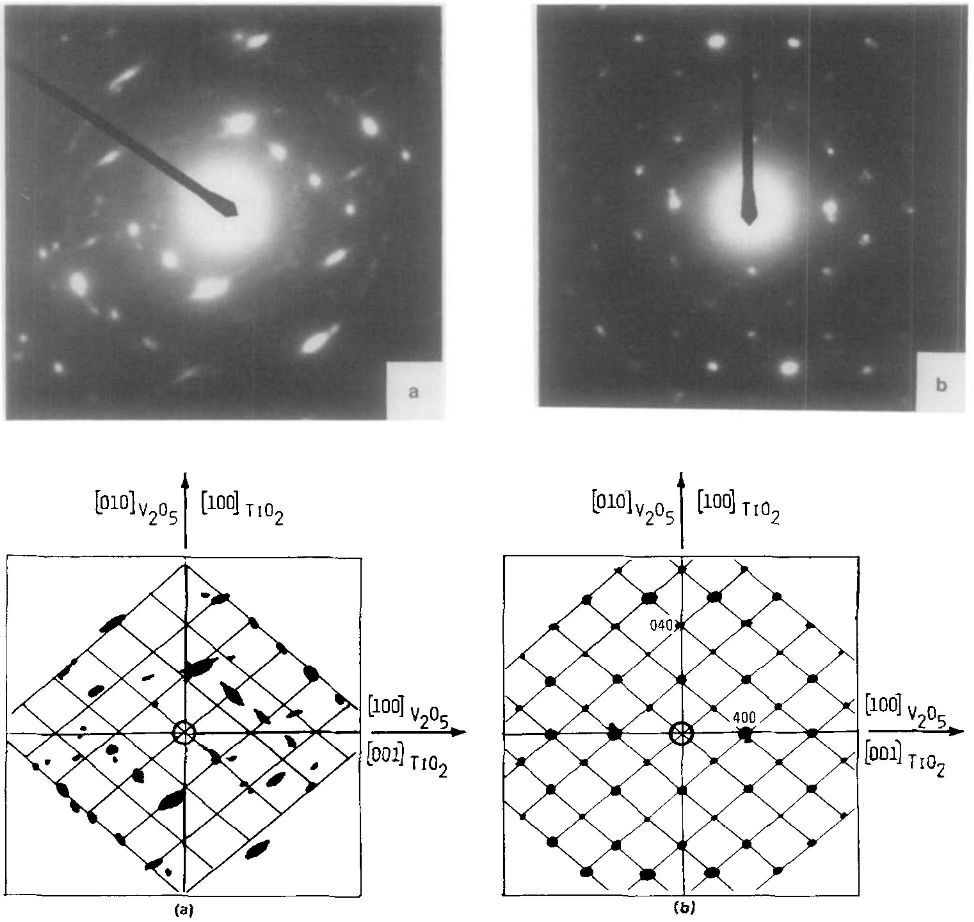

FIG. 8. Typical electron diffraction patterns from $V_2O_5$–$TiO_2$(anatase) system (specimens III) (continued). (a) New phase in formation (streaking indicates planar structural transition). (b) New phase completed (electron diffraction pattern associated with micrograph 6c. (400) spot marked is also the $V_2O_5$ (400) spot; (040) spot is the $V_2O_5$ (020) spot.

contrary the formation of new phases was distinctly related to the reactivity of the $V_2O_5$–$TiO_2$(anatase) system.

The occasional evidences of relative crystallographic orientation following the postulated matching scheme seemed to further support the main idea that the reactivity of the $V_2O_5$–$TiO_2$(anatase) system is an effect of interfacial *coherence*. Coherence which in the redox conditions of oxidation catalysis (less severe than the electron beam) would account for the fact that the system becomes active and selective in the stationary state without relaxation.

More work is needed to indisputably prove the formation of coherent interfaces. On the other hand the concept of coherence seems to be the only plausible explanation of the recognized fact that the condition of crystallographic fit constitutes a simple and reliable *criterion* in the determination of a particular catalyst, satisfactory in terms of activity, selectivity, and life.

Of course, it cannot be concluded by simple extrapolation that the same interfacial phenomena exist in $V_2O_5$–$TiO_2$(anatase) catalysts industrially prepared. However, on the one hand the same kind of anatase is involved in both cases; on the other hand, one sees no serious reason for the $V_2O_5$ formed through aqueous precipitation, dessication, and calcination, to develop under a morphology different from the usually prevailing one. These considerations lead us to assume that interfacial relationships comparable to those discussed above in our particular system exist also in the same way in industrial catalysts.

## Acknowledgment

This work was partly supported by the European CODEST program (Action de Stimulation à la Recherche).

## References

1. A. Vejux and P. Courtine, *J. Solid State Chem.* **23,** 93 (1978).
2. M. Inomata, A. Miyamoto, and Y. Murakami, *J. Phys. Chem.* **85,** 2372 (1981).
3. M. Inomata, K. Mori, A. Miyamoto, T. Ui, and Y. Murakami, *J. Phys. Chem.* **87,** 754 (1983).
4. D. J. Hucknall, *in* "Selective Oxidation of Hydrocarbons," Academic Press, New York, 1974.
5. D. J. Cole, C. F. Cullis, and D. J. Hucknall, *J. Chem. Soc. Faraday Trans.* **72,** 2185 (1981).
6. G. C. Bond and K. Bruckman, *Faraday Disc. Chem. Soc.* **72,** 235 (1982).
7. G. C. Bond, A. J. Sarkany, and C. D. Parfitt, *J. Catal.* **57,** 476 (1979).
8. G. C. Bond and P. Konig, *J. Catal.* **77,** 809 (1982).
9. M. Inomata, A. Miyamoto, T. Ui, K. Kobayashi, and Y. Murakami, *Ind. Eng. Chem. Prod. Res. Rev.* **21,** 424 (1982).
10. C. F. Cullis and D. J. Hucknall, *Catalysis* **5,** 273 (1985).
11. M. Gazior and B. Grzybowska, *Bull. Acad. Polon. Sci. Ser. Sci. Chim.* **27,** 835 (1985).
12. B. Grzybowska, Y. Barbaux, and J. P. Bonelle, *J. Chem. Res.* (*S*), 650 (1980).
13. R. Kozlowski, R. Pettifer, and J. M. Thomas, *J. Chem. Phys.* **87,** 5176 (1983).
14. I. E. Wachs and S. S. Chan, *J. Catal.* **91,** 366 (1985).
15. F. Roozeboom, M. C. Mittlemeijer-Hazeleger, J. A. Moulijn, J. Medena, V. H. J. de Beer, and P. J. Gellings, *J. Phys. Chem.* **84,** 2783 (1980).
16. P. Courtine, *in* "American Chemical Society Symposium Series, Vol. 279-3, "The Role of Solid State Chemistry in Catalysis" (R. K. Grasselli and J. F. Brazdil, Eds.), p. 37, American Chemical Society, Washington, D.C., 1985.
17. P. Courtine and A. Vejux, *C.R. Acad. Sci. C* **286,** 135 (1978).
18. (*a*) J. G. Eon and P. Courtine, *C.R. Acad. Sci. C.* **288,** 17 (1979); (*b*) J. G. Eon and P. Courtine, *J. Sol. State Chem.* **32,** 67 (1980).
19. Private communication.
20. R. G. Wyckoff, *in* "Crystal Structure," Vols. I, II, Interscience, New York, 1964.
21. H. G. Bachmann, F. R. Ahmed, and W. H. Barnes, *Z. Kristallogr.* **115,** 110 (1961).
22. B. G. Hyde and L. A. Bursill, *in* "The Chemistry of Extended Defects in Non-metallic Solids" (Le Roy Eyring and Michael O'Keefe, Eds.), p. 347, North-Holland, Amsterdam, 1970.
23. R. J. D. Tilley and B. G. Hyde, *J. Phys. Chem. Solids* **31,** 1613 (1970).
24. B. G. Hyde and R. J. D. Tilley, *Phys. Status Solidi* **2,** 749 (1970).
25. G. Grymonprez, L. Fiermans, and J. Vennick, *Acta Crystallogr. Sect. A* **33,** 834 (1977). (See also references cited and gathered therein, particularly Colpaert or Theobald *et al.*)
26. J. S. Anderson, *in* "Reaction Paths and Microstructure in Crystals," Proceedings, 7th Int. Symp. Reactivity on Solids, Bristol, p. 1–22, Chapman & Hall, London, 1972.
27. A. R. Ubbelohde, *J. Chim. Phys.* **62,** 33 (1966).
28. A. R. Ubbelohde, *Trans. Farad. Soc.* **33,** 1198 (1937).
29. E. Bordes and P. Courtine, *J. Catal.* **57,** 236 (1979).
30. P. Courtine, *in* "American Chemical Society Symposium Series," Vol. 279-3, "The Role of Solid State Chemistry in Catalysis" (R. K. Grasselli and J. F. Brazdil, Eds.), p. 47, American Chemical Society, Washington, D.C., 1985.
31. J. Haber, *Pure Appl. Chem.* **56,** 1663 (1984).